(to appear in the Astronomical Journal)

The Universality of the Fundamental Plane of E and S0 Galaxies. Spectroscopic Data[1]

Marco Scodeggio[2], Riccardo Giovanelli and Martha P. Haynes
Center for Radiophysics and Space Research and National Astronomy and Ionosphere Center[3],
Cornell University, Ithaca, NY 14853
mscodegg@eso.org
riccardo, haynes@astrosun.tn.cornell.edu

ABSTRACT

We present here central velocity dispersion measurements for 325 early-type galaxies in eight clusters and groups of galaxies, including new observations for 212 galaxies. The clusters and groups are the A262, A1367, Coma (A1656), A2634, Cancer and Pegasus clusters, and the NGC 383 and NGC 507 groups. The new measurements were derived from medium dispersion spectra, that cover 600 Å centered on the Mg Ib triplet at $\lambda \sim 5175$. Velocity dispersions were measured using the Tonry & Davis cross-correlation method, with a typical accuracy of 6%. A detailed comparison with other data sources is made.

Subject headings: distance scale — galaxies: distances and redshifts — galaxies: elliptical and lenticular — galaxies: fundamental parameters — galaxies: kinematics and dynamics

1. Introduction

This is the fourth in a series of papers (Scodeggio, Giovanelli & Haynes 1997a,b; hereafter Paper I and Paper II; Scodeggio, Giovanelli & Haynes 1998a; hereafter Paper III) devoted to a

---

[1]Work based in part on observations obtained with the Hale 200" telescope at the Palomar Observatory. These observations were made as part of a continuing collaborative agreement between the California Institute of Technology and Cornell University.

[2]Present address: European Southern Observatory, Karl-Schwarzschild-Straβe 2, D-85748, Garching bei München, Germany.

[3]The National Astronomy and Ionosphere Center is operated by Cornell University under a cooperative agreement with the National Science Foundation.

study of the universality of the Fundamental Plane (FP) relation of early-type galaxies (Djorgovski & Davis 1987; Dressler *et al.* 1987). The universality of the FP, and of other distance indicator relations like the Tully-Fisher (TF) relation (Tully & Fisher 1977), is the fundamental assumption behind their use, but this assumption cannot be taken for granted, because of the existence of well known environmental effects that can link the evolution of a galaxy to the properties of its surrounding environment. It is therefore important to obtain an observational verification of such universality (discussions on this subject are presented by Djorgovski, de Carvalho & Han 1988; Guzmán *et al.* 1992; Jørgensen, Franx & Kjærgaard 1996; Schroeder 1996; Giovanelli *et al.* 1997b; Paper I).

In this series, we present the results of a FP study of eight clusters, with the aim of obtaining a quantitative verification of the FP universality through a comparison of accurate distance estimates obtained using both the FP and the TF relations. These clusters are taken from the list of clusters studied by Giovanelli *et al.* (1997a,b) using the TF relation, and are the Coma, A1367, A2634, A262, Cancer, and Pegasus clusters, and the NGC 507 and NGC 383 groups. In this paper we present spectroscopic data, necessary for building the FP relation, for 325 galaxies, including new observations for 212 galaxies, while Paper III contains I band CCD photometric data, and describes the cluster selection and membership criteria adopted for the FP work. In successive work (Scodeggio, Giovanelli & Haynes 1998b) we will discuss the properties of the I band FP relation, and the comparison between TF and FP distance estimates for the clusters in our sample.

This papers is organized as follows: sections 2, 3, and 4 present our new spectroscopic observations and the adopted data reduction procedures. Sections 5 and 6 present the complete spectroscopic sample that will be used in the FP work, and the internal and external comparisons used to assess the quality of our new measurements.

2. Observations

New spectroscopic observations for this work were obtained during 8 observing runs with the Hale 5m telescope of the Palomar Observatory, from September 1992 to September 1996. Table 1 summarizes these observing runs, and gives the parameters of the relative instrumental setups. During all runs the red camera of the Double Spectrograph (Oke & Gunn 1982) was used with a 1200 lines/mm grating, to produce spectra with a dispersion of approximately 0.82 Å per pixel (except in runs 7 and 8, when a different CCD chip was mounted on the camera, and the dispersion was approximately 0.66 Å per pixel). This resulted in a spectral coverage of approximately 600 Å, from 5000 to 5600 Å, including the Mg Ib lines at $\lambda \sim 5175$. The spectral resolution, measured both from the width of the calibration lamps lines, and from the width of the peak in the autocorrelation function of the spectrum of velocity standard stars, was approximately 2.2 Å (FWHM) for all runs. This is equivalent to a velocity resolution of 129 $\mathrm{km\,s^{-1}}$ at 5300 Å. All observations were obtained with a 2 arcsec wide slit, while the length of the slit was 128 arcsec. The slit orientation was kept in the East-West direction, unless a close pair of galaxies could be observed at once with the proper slit orientation. Galaxies were visually centered in the slit using the acquisition camera of the Double Spectrpgraph. Integration times varied between 10 and 90 minutes, depending on the brightness of the galaxy. The median integration time was 30 minutes. He-Ne-Ar lamp spectra were obtained before and after each galaxy observation, to provide wavelength calibration. Late G and early K type giant stars were observed each night to serve as templates for radial velocity and velocity dispersion determinations. To maximize the signal-to-noise ratio in these template spectra, the star observations were obtained with 30-120 sec integrations, while trailing the star along the slit. This allowed to spread the light on a large area of the CCD chip without saturating the image.

3. Basic data reduction and wavelength calibration

The data reduction process was performed entirely using standard IRAF[4] procedures. All frames were bias-subtracted and flat-fielded, using dome flats. The number of pixels affected by cosmic rays hits was small in all the frames, and they were blanked during a phase of visual inspection of all frames. Because most of the spectroscopic observations were obtained in non photometric conditions, no attempt was made to obtain a flux calibration for any of the derived spectra.

Wavelength calibration was performed in a two-step process. First, the He-Ne-Ar lamp spectra frames obtained before and after each galaxy spectrum were used to obtain a two-dimensional dispersion solution, where a wavelength value is assigned to each pixel in the CCD frame. Typically 12-14 spectral lines, spread uniformly over the entire wavelength range, were used in the fit. The rms deviations between fitted and true wavelength were of the order of 0.06–0.1 Å in the central portion of the frames (where the galaxy spectra are positioned), and increased up to 0.25 Å at the edges of the frame, due to the camera astigmatism and to focusing problems caused by the less than perfect flatness of the CCD chip. Single line deviations from the best fit solutions were always less than 0.3 Å. An uncertainty in the wavelength calibration of 0.1 Å at 5300 Å translates into a velocity uncertainty of 5.6 $\mathrm{km\,s^{-1}}$. The CCD chip used for runs 7 and 8 does not have focusing problems, and therefore the rms uncertainty in the calibration of the spectra obtained in those runs was of the order of 0.08 Å, uniformly across the entire frame. The two-dimensional dispersion solutions were applied to the galaxy spectral frames, so that all pixels in one row of the corrected CCD frame were characterized by the same wavelength. Finally the two strong night-sky lines at 5460.7 Å (Hg) and 5577.4 Å (OI) were used to check the absolute wavelength calibration. The 1-σ dispersion in the measured wavelengths of these lines was approximately 0.08 Å. A small fraction (2-3%) of the frames showed large deviations ($> 4\sigma$) in the wavelength measured for the

[4]IRAF (Image Reduction and Analysis Facility) is distributed by the National Optical Astronomy Observatories, which are operated by the Association of Universities for Research in Astronomy (AURA), Inc., under a cooperative agreement with the National Science Foundation.

two sky lines. For these cases the original dispersion solution was rigidly shifted to bring the two lines into agreement with their expected wavelengths.

An independent check on the wavelength calibration was performed using the velocity standard star spectra. Radial velocities were measured repeatedly using all star spectra obtained in the different runs. Using in turn one star as velocity standard and all others as unknown, radial velocities were derived, to be compared with the known radial velocity of each star. The rms deviations between the measured and the known velocities were between 6.0 and 8.5 $\mathrm{km\,s^{-1}}$, when spectra obtained during a single run only were considered, and approximately 9 $\mathrm{km\,s^{-1}}$ when spectra from all runs were considered. This result is in good agreement with the calibration uncertainty derived from the sky lines measurements. Therefore 9 $\mathrm{km\,s^{-1}}$ is an estimate of the overall accuracy we can achieve with this spectroscopic data set.

4. Determination of the spectroscopic parameters

During the last twenty years a number of methods have been developed to perform velocity dispersion measurements as objectively as possible (see for example Sargent *et al.* 1977; Tonry & Davis 1979; Franx, Illingworth & Hechman 1989; Bender 1990). These methods are all based on the comparison between the spectrum of the galaxy whose velocity dispersion is to be determined, and a fiducial spectral template. This can be either the spectrum of an appropriate star, with spectral lines unresolved at the spectral resolution being used, or a high signal-to-noise spectrum of a galaxy with known velocity dispersion. There are small but in principle significant differences among these methods, but in practice all methods seem to give results in good relative agreement, when applied to spectra with high signal-to-noise ratio, making the choice of one particular method a non critical issue.

In this work, quantitative measurements on the spectra have been obtained using the cross-correlation technique of Tonry & Davis (1979), implemented in the IRAF task *fxcor*. The basic assumption behind this and other similar methods is that the spectrum of an elliptical galaxy (and also of the bulge of a disk galaxy) is well approximated by the spectrum of its most luminous stars (K0–K1 giants), modified only by the effects of the stellar motions inside the galaxy. Since these motions introduce just a Doppler shift in the stellar spectra, the galaxy spectrum is given by the convolution of the spectrum of a K giant star with the line of sight stellar velocity distribution (LOSVD). Therefore the LOSVD can be obtained with a deconvolution process from the galaxy spectrum and a suitable stellar template. Since cross-correlation and convolution are two related operators, the Tonry & Davis algorithm uses cross-correlation as a computational tool to derive the LOSVD. The procedure takes advantage of the fact that the Fourier transform of a convolution, or of a cross-correlation, reduces to a product between individual functions' transforms.

The one-dimensional galaxy spectra used for the radial velocity and velocity dispersion measurements were extracted from the two-dimensional wavelength calibrated frames using a 6 arcsec wide window, centered on the peak of the galaxy continuum light. This, combined with the 2 arcsec slit aperture, provides a final effective aperture of 6 x 2 arcsec for all the galaxy observations. The stellar templates were obtained averaging the signal over 20–30 pixels in the spatial dimension at all wavelengths, to produce spectra with a signal to noise ratio greater than 200. Before computing the Fourier transforms and the cross-correlation function, all spectra were continuum-subtracted, normalized, end-masked with a cosine bell function, and re-binned to a logarithmic wavelength scale. The final velocity dispersion measurements have been obtained by averaging the determinations obtained with five different stellar templates, of spectral types between G9 and K2. No significant dependence of the measurements on the template star spectral type was observed.

4.1. The Effect of the Noise

Because of the limited signal-to-noise (S/N) ratio of the spectra being analyzed, and also to facilitate comparisons with other studies, we have constrained the deconvolution procedure by assuming the LOSVD to be Gaussian, and therefore characterized by two parameters only: a mean redshift z and a velocity dispersion σ. The reliability of this method has been tested using simulations with synthetic spectra. Stellar templates have been broadened with Gaussian profiles of known width to simulate a large range of velocity dispersions, and noise has been added to the resulting spectra, to reproduce the S/N characteristic of the galaxy spectra. Then velocity dispersions have been measured using the original stellar spectrum as a template. These tests show that *fxcor* produces an overestimate of the velocity dispersion, at the 4-5% level, while no bias is present in the measurement of radial velocities. The raw measurements have been therefore corrected to remove this effect. To a first approximation, this effect appears to be independent of the S/N ratio of the input spectrum, but no simulation was performed using spectra with S/N ratio lower than 20.

If the true LOSVD is approximately Gaussian, then the statistical uncertainty with which the velocity dispersion is obtained is a function of the S/N ratio of the galaxy spectrum only, since the S/N ratio in the template spectrum is many times higher than that of the galaxy spectrum (see Tonry & Davis 1979 for details). An estimate of the amplitude of this uncertainty was obtained using synthetic spectra with added noise. It was found that a good approximation to the value of the uncertainty is given by the relation $\epsilon_{\log\sigma} \simeq 1.1/(S/N)$. The median uncertainty on the radial velocity determination is 13 $\mathrm{km\,s^{-1}}$, and on the velocity dispersion is 6%.

As a visual guide to the quality of the data presented in this work, we show in Figure 1 the spectra of 6 different galaxies. These are divided into two groups, and all three galaxies in one group have very similar velocity dispersion (approximately 140 and 230 $\mathrm{km\,s^{-1}}$, respectively), but their spectra have different S/N ratio. These spectra were chosen to provide an example of a spectrum at the upper quartile, median, and lower quartile in the distribution of S/N values for the spectra in our dataset.

4.2. The Effect of Rotation

Galaxy one-dimensional spectra were extracted using a 6 arcsec aperture, which can bracket a fairly large portion of the target galaxy, especially for more distant clusters. Therefore galaxy rotation, if present, can contribute some broadening of the spectral lines and bias the velocity dispersion measurements. We thus use the galaxy two-dimensional spectra to estimate the galaxy rotation velocity, and gauge whether a correction of the velocity dispersion measurements is necessary. A 5 point rotation curve within the 6 arcsec aperture (10 pixels) has been obtained for each galaxy, using 5 one-dimensional spectra, extracted using 2-pixel wide apertures positioned side by side. Using the cross-correlation method, individual mean velocities can be obtained for the 5 spectra. The differences in the radial velocities measured between each one of the four lateral spectra and the one measured in the central 2 pixels define the projection of the galaxy rotation curve along the slit.

The contribution of a given rotation to the broadening of the spectral lines has been estimated using a very simple model. A galaxy spectrum has been simulated combining 5 copies of a stellar template, broadened with a Gaussian of fixed width, and shifted to reproduce the 5 velocities in the rotation curve. The weights used in the combination have been derived from the relative intensities in the continuum of the 5 one-dimensional galaxy spectra used to obtain the rotation curve. The comparison of the velocity dispersion in the simulated spectrum with the one used to broaden the stellar template spectra provides an estimate of the amount of broadening due to the rotation.

Given the accuracy with which radial velocities can be measured, and the small number of points used to define the rotation curve, rotation velocities smaller than $\simeq$20 km s^{-1} cannot be reliably measured. Within the sample presented here, 75 galaxies do not show detectable rotation. The remaining 137 have a median rotation velocity of 40 km s^{-1}, with the largest measured velocity being 130 km s^{-1}. Note that we had no a priori information on the position angle of the axis of rotation of each galaxy. This rotation is responsible for an average broadening of the LOSVD of $\simeq$4%, with a maximum of $\simeq$9% for the largest rotation velocities.

4.3. Aperture Correction

Because of radial gradients in the stellar velocity dispersion within early-type galaxies, the velocity dispersion measured in a given galaxy depends on the size of the aperture that is used to extract its spectrum. When spectra are obtained with a fixed aperture size (in arcsec), this aperture covers regions of different physical size (in kiloparsec) on galaxies at different distances, and this produces biased velocity dispersion measurements. Therefore fixed aperture measurements must be corrected to a standard, distance independent, aperture size. Here all measurements are corrected to the value one would obtain for a galaxy at the distance of the

Coma cluster, using the relation derived by Jørgensen, Franx & Kjærgaard (1995)

$$\log \frac{\sigma_{ap}}{\sigma_{norm}} = -0.04 \ \log \frac{r_{ap}}{r_{norm}} = -0.04 \ \log \frac{d}{d_{Coma}} \tag{1}$$

where σ_{ap} and σ_{norm} are the measured and corrected velocity dispersion, r_{ap} and r_{norm} are the projected angular size of a given length at the distance of the observed galaxy and at the reference distance used for the normalization, and d and d_{Coma} are the distance of the cluster to which the given galaxy belongs, and that of the Coma cluster. Distances are derived from the cluster redshifts, in the CMB reference frame.

5. The spectroscopic sample

Spectroscopic data for early-type galaxies in 8 clusters and rich groups of galaxies are presented here. These are the NGC 383 group, NGC 507 group, A262, Cancer, A1367, Coma (A1656), Pegasus, A2634. A short discussion on their properties, and on the membership criteria we used to assign galaxies to these clusters, is presented in Paper III. Our spectroscopic sample is composed of two partly overlapping datasets: our own observations, discussed in the previous sections, for a total of 212 galaxies, and a compilation of data from the literature, which includes 152 galaxies. For the Coma cluster, most of the data come from the literature, while for the other clusters most of the data are new. In all cases we have tried to complement the existing observations in order to obtain approximately flux limited samples, while having enough overlap with those observations, as to compare the different velocity dispersion scales.

5.1. New observations

The criteria adopted to select galaxies for our spectroscopic observations were as follows: CGCG magnitudes (Zwicky *et al.* 1963-1968) were used for the sample selection, if available. Otherwise our own eye estimates, calibrated on the same scale, were used. All galaxies with morphological type E, S0, and S0a were included in the sample. A few objects, that were originally classified as S0 or S0a, were later classified Sa on the basis of the CCD imaging (see Paper III), but they were left in the sample if a spectrum had already been taken. Only galaxies with previously available redshift measurements, so that their cluster membership was already known, were targeted for observations.

No particular criterion was used to select the objects that would provide an overlap with already available datasets. An effort was made, however, to cover as large an interval of velocity dispersions as possible.

Table 2 presents the relevant parameters for the 212 objects for which we have obtained spectroscopic observations. Only the first page is presented herefor guidance regarding its form

and content . The table is available in its entirety in digital form on the Journal Electronic Edition, or from the authors. The table is organized as follows:
Col. 1: Galaxy name: if the galaxy is listed in the UGC catalog (Nilson 1973), the UGC number is given; if not, our internal coding number, from the private galaxy catalog of Giovanelli & Haynes referred to as the AGC, is given.
Cols. 2 and 3: the NGC or IC number, if available, and the CGCG field and ordinal number within that field, if the galaxy is listed in the CGCG (Zwicky *et al.* 1963-1968). For galaxies in the Coma cluster that are not listed in either one of those catalogs, the Dressler number (Dressler 1980) is given, if available.
Cols. 4 and 5: Right Ascension and Declination, in 1950.0 epoch.
Col. 6: morphological type code, in the RC3 (de Vaucouleurs *et al.* 1991) scheme (-5 for E, -2 for S0, 0 for S0a). Morphological types were derived from joint inspection of the blue plates of the Palomar Observatory Sky Survey (POSS), and of the CCD images discussed in Paper III.
Col. 7: Measured heliocentric velocity, in $\mathrm{km\,s^{-1}}$.
Col. 8: Measured stellar velocity dispersion, in $\mathrm{km\,s^{-1}}$.
Col. 9: Measured rotation velocity, in $\mathrm{km\,s^{-1}}$. If no data is present, the spectrum had to low a S/N ratio to perform the measurement.
Col. 10: Velocity dispersion, in $\mathrm{km\,s^{-1}}$, corrected for galaxy rotation.
Col. 11: Logarithm of the rotation-corrected velocity dispersion.
Col. 12: Uncertainty on the logarithm of the velocity dispersion.
Col. 13: Aperture-corrected logarithm of the velocity dispersion.
Col. 14: A reference code indicates if other velocity dispersion measurements were available in the literature, and their source. If an asterisk appears in this column, special comments on the object are included at the foot of the table.

A subset of these data has already been published in Paper I, limited to galaxies in the Coma and A2634 clusters. Since then, a few galaxies have been reobserved, and the data combined to obtain new measurements of the relevant photometric parameters. The data presented here therefore supersede that previous report.

5.2. Data from the literature

Velocity dispersion measurements are available in the literature for each of the clusters in our sample. The number is large only in the case of the Coma cluster, where measurements from Dressler (1987), Davies *et al.* (1987), Faber *et al.* (1989), and Lucey *et al.* (1991) are available for a total of 103 galaxies, and in the case of A2634, where measurements from Lucey *et al.* (1997) are available for 37 galaxies. For the remaining clusters, we have found data in Faber *et al.* (1989) for 6 galaxies in A262, 7 galaxies in A1367, 1 galaxy in Cancer, 4 galaxies in Pegaus, 12 galaxies in the NGC 507 and NGC 383 groups. For the brightest galaxy in some of the clusters multiple measurements from various sources are available (see the footnotes to Table 2). In all clusters, we have limited our search to galaxies for which we have obtained I band photometric measurements (see Paper III). Therefore a larger spectroscopic dataset than the one reported here might be available in some cases. Table 3 lists the relevant parameters for the 170 objects for which data are derived from the literature. Only the first page is presented here; the entire table is available in digital form on the Journal Electronic Edition, or from the authors. The table is organized as follows:

Cols. 1 to 6: same as in Table 2.
Col. 7: Heliocentric velocity, in $\mathrm{km\,s^{-1}}$.
Col. 8: Stellar velocity dispersion, in $\mathrm{km\,s^{-1}}$.
Col. 9: Logarithm of the velocity dispersion.
Col. 10: Uncertainty on the logarithm of the velocity dispersion. A common value for each main dataset was adopted, corresponding to the typical uncertainty quoted by the authors.
Col. 11: Aperture-corrected logarithm of the velocity dispersion.
Col. 12: Reference code.

6. Internal and external comparison

Repeated observations of a fraction of the galaxies in our sample provide the opportunity to evaluate the internal consistency of the spectroscopic measurements. However, the number of repeated observations is rather small, because spectroscopic observations are quite expensive in terms of telescope time. In total, 27 pairs of observations are available for an internal comparison. Table 4 lists the results of the comparison of radial velocity and velocity dispersion. Mean statistical uncertainties associated with the derivation of those parameters are included in the Table, multiplied by a $\sqrt{2}$ factor to allow a direct comparison with the rms scatter in the observations (assuming equal error contributions to the rms scatter). The rms scatter in the radial velocity comparison (see Figure 2a) is surprisingly large (29 $\mathrm{km\,s^{-1}}$), but it is mostly due to just 2 galaxies. After removing these extreme cases the scatter is reduced to 19 $\mathrm{km\,s^{-1}}$, in agreement with the statistical uncertainties on the radial velocity determinations. Unfortunately with such small number statistics it is difficult to decide whether these 2 objects are truly outliers. However we point out that in bot cases one of the two spectra being compared has an extremely low signal-to-noise ratio, and therefore the uncertainty on the determination of the corresponding spectroscopic parameters is expected to be large.

The comparison of the velocity dispersions is presented in Figure 2b, and shows that, as expected, the accuracy of the dispersion determinations for very low velocity dispersion objects ($\sigma < 100\,\mathrm{km\,s^{-1}}$) is lower than that for higher velocity dispersion objects. The rms scatter measured for the 6 low velocity dispersion objects is in fact more than twice as large as the one measured for the remaining 21 objects. When these low velocity dispersion objects are removed from the sample, we find a fair agreement between the expected uncertainties and the observed dispersion in the measurements.

The absolute consistency of the velocity dispersion measurements is evaluated through a comparison with measurements taken from the literature. There are 62 observations for 57 galaxies for which this comparison is possible. The results of such a comparison are presented in Table 5 and in Figure 3, where the difference (us - literature) is plotted vs. the mean value of the velocity dispersion, derived combining the two measurements. Five extremely discrepant objects are removed from this comparison. For two objects the measurement we have obtained for their velocity dispersion is affected by a large uncertainty. For the remaining three no easy explanation for the observed discrepancy is available. It is clear that there is good agreement with the observations of Dressler (1987), Davies *et al.* (1987), and Faber *et al.* (1989), collectively indicated as 7S in Table 5, and also with the observations of Lucey *et al.* (1997). No significant offset is present, and the observed rms scatter of the differences in the values of $\log\sigma$ is in good agreement with an expected one, based on the 6% median uncertainty of our measurements, and on an average 10% uncertainty for the measurements in the literature. A small discrepancy is present when the Coma cluster observations of Lucey *et al.* (1991) are considered, but the sample is probably too small to derive robust conclusions. We notice that the comparison between Lucey *et al.* (1991) and Faber *et al.* (1989) datasets, based on a larger sample of galaxies, shows good relative agreement (see Lucey *et al.* 1991). Given the good agreement between the different datasets, all measurements presented in Table 2 and 3 will be merged for the FP work that will be discussed in Scodeggio *et al.* (1998b).

We would like to thank John Henning, Mike Doyle, Dave Tennant, and Bob Thicksten for their technical support during the various observing runs at Palomar, Juan Carrasco for his masterful handling of many observing nights, and Gary Wegner for helpful discussions on the comparison between different spectroscopic datasets. This research has made use of the NASA/IPAC Extragalactic Database (NED) which is operated by the Jet Propulsion Laboratory, California Institute of Technology, under contract with the National Aereonautics and Space Administration. This research is part of the Ph.D. Thesis of MS, and is supported by the NSF grants AST94–20505 and AST96–17069 to RG and AST95–28860 to MPH.

REFERENCES

Bender, R. 1990, A&A, 229, 441

Davies, R.L., & Illingworth, G. 1983, ApJ, 266, 516

Davies, R.L., Burstein, D., Dressler, A., Faber, S.M., Lynden-Bell, D., Terlevich, R.J., & Wegner, G. 1987, ApJS, 64, 581

de Vaucouleurs, G., de Vaucouleurs, A., Corwin, H.G., Buta, R., Paturel, G., & Fouqué, P. 1991, "Third Reference Catalogue of Bright Galaxies" (New York: Springer) (RC3)

Djorgovski, S.G., & Davis, M. 1987, ApJ, 313, 59

Djorgovski, S.G., De Carvalho, R.R., & Han, M.S. 1988, in "The Extragalactic Distance Scale", ed. S. van den Bergh & J. Pritchet, p. 329

Dressler, A. 1980, ApJS, 42, 565

Dressler, A. 1987, ApJ, 317, 1

Dressler, A., Lynden-Bell, D., Burstein, D., Davies, R.L., Faber, S.M., Terlevich, R.J., & Wegner, G. 1987, ApJ, 313, 42

Faber, S. M., & Jackson, R. E. 1976, ApJ, 204, 668

Faber, S.M., Wegner, G., Burstein, D., Davies, R.L., Dressler, A., Lynden-Bell, D., & Terlevich, R.J. 1989, ApJS, 71, 173

Fisher, D., Illingworth, G., & Franx, M. 1995, ApJ, 438, 539

Franx, M., Illingworth, G., & Hechman, T. 1989, ApJ, 344, 613

Giovanelli, R., Haynes, M.P., Herter, T., Vogt, N.P., da Costa, L.N., Freudling, W., Salzer, J.J. and Wegner, G. 1997a, AJ, 113, 22 (G97a)

Giovanelli, R., Haynes, M.P., Herter, T., Vogt, N.P., da Costa, L.N., Freudling, W., Salzer, J.J. and Wegner, G. 1997b, AJ, 113, 53 (G97b)

Guzmán, R., Lucey, J.R., Carter, D., & Terlevich, R.J. 1992, MNRAS, 257, 187

Jørgensen, I., Franx, M., & Kjærgaard, P. 1995, MNRAS, 276, 1341

Jørgensen, I., Franx, M., & Kjærgaard, P. 1996, MNRAS, 280, 167

Lucey, J.R., Guzmán, R., Carter, D., & Terlevich, R.J. 1991, MNRAS, 253, 584

Lucey, J.R., Guzmán, R., Steel, J., & Carter, D., 1997, MNRAS, 287, 899

Malumuth, E.M., & Kirshner, R.P. 1981, ApJ, 251, 508

Nilson, P. 1973, "Uppsala General Catalogue of Galaxies" (Uppsala Astron. Obs. Ann., Vol. 6) (UGC)

Oegerle, W.R., & Hoessel, J.G. 1991, ApJ, 375, 15

Oke, J.B., & Gunn, J.E. 1982, PASP, 94, 586

Sargent, W.L.W., Schechter, P.L., Boksenberg, A., & Shortridge, K., 1977, ApJ, 212, 326

Schroeder, A., 1996, PhD Thesis, Univ. of Basel

Scodeggio, M., Giovanelli, R., & Haynes, M.P. 1997a, AJ, 113, 101 (Paper I)

Scodeggio, M., Giovanelli, R., & Haynes, M.P. 1997b, AJ, 113, 2087 (Paper II)

Scodeggio, M., Giovanelli, R., & Haynes, M.P. 1998a, submitted to AJ(Paper III)

Scodeggio, M., Giovanelli, R., & Haynes, M.P. 1998b, in preparation

Tonry, J.L. 1984, ApJ, 279, 13

Tonry, J.L. 1985, AJ, 90, 2431

Tonry, J.L., & Davis, M. 1979, AJ, 84, 1511

Tonry, J.L., & Davis, M. 1981, ApJ, 246, 666

Tully, R.B., & Fisher, J.R. 1977, A&A, 54, 661

Zwicky, F., Herzog, E., Wild, P., Karpowicz, M., & Kowal, C. 1961–1968, "Catalogue of Galaxies and Clusters of Galaxies" (Pasadena: California Institute of Technology)

Table 1: Spectroscopic observing runs

	Runs 1–6	Runs 7–8
Telescope	Palomar 5m	Palomar 5m
Instrument	DS-red camera	DS-red camera
CCD	TI 305 #8	Tek1024
Pixels	800 x 300	1024 x 300
Read-out noise	11 e^-	7.5 e^-
Gain	1.7 e^-/DU	2.0 e^-/DU
Spatial scale	0.61 ″/pixel	0.46 ″/pixel
Slit aperture	2 arcsec	2 arcsec
Grating	1200 l/mm	1200 l/mm
Dispersion	0.82 Å/pixel	0.66 Å/pixel
Spectr. resol.	2.2 Å (129 km/s)	2.2 Å (129 km/s)
Wavelength cover.	4960-5620 Å	4960-5660 Å

	Run 1	Run 2	Run 3	Run 4
Dates	Sep. 23-26 1992	Sep. 17-20 1993	Mar. 3-6 1994	Apr. 28-29 1994
Nights used	2	4	3	1
Nr. of galaxies	16	64	31	6

	Run 5	Run 6	Run 7	Run 8
Dates	Sep. 6-12 1994	Aug. 23-25 1995	Mar. 19-20 1996	Sep. 20 1996
Nights used	7	3	1	1
Nr. of galaxies	72	28	5	8

Table 4. Spectroscopic data quality: internal comparison

Parameter	N_{gal}	mean difference	rms scatter	mean uncertainty
V_{hel} (all)	27	5.8	28.9	18.0
V_{hel} (2 most discr. excluded)	25	-2.2	19.3	18.0
$\log \sigma$ (all)	27	0.002	0.055	0.031
$\log \sigma$ ($\sigma > 100$ km s^{-1})	21	0.002	0.041	0.037
$\log \sigma$ ($\sigma < 100$ km s^{-1})	6	0.001	0.096	0.037

Table 5. Spectroscopic data quality: external comparison

Parameter	N_{gal}	mean difference	rms scatter
$\log \sigma$ (all)	56	-0.004	0.053
$\log \sigma$ (7S)	29	-0.004	0.050
$\log \sigma$ (L97)	21	-0.001	0.057
$\log \sigma$ (L91)	6	-0.015	0.056

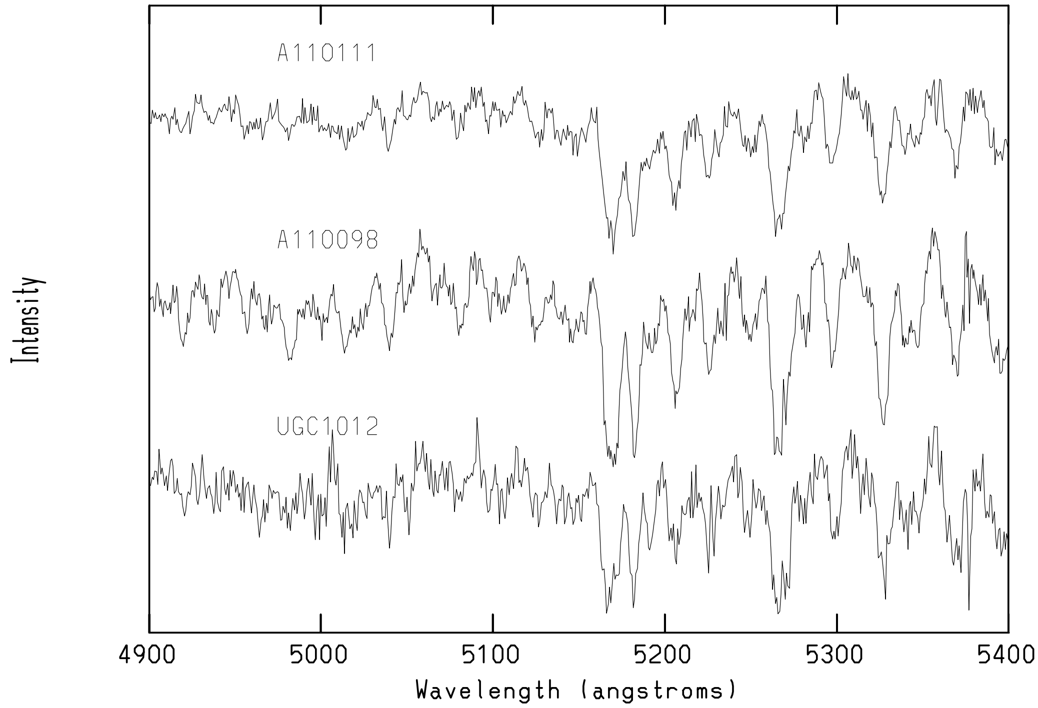

Fig. 1.— Spectra of 6 different galaxies in our data-set. These are divided into two groups, and all three glaxies in one group have very similar velocity dispersion (approximately 140 and 230 km s^{-1}, respectively), but their spectra have different S/N ratio. These spectra were chosen to provide an example of a spectrum at the upper quartile, median, and lower quartile (top to bottom) in the distribution of S/N values for the spectra in our data-set.

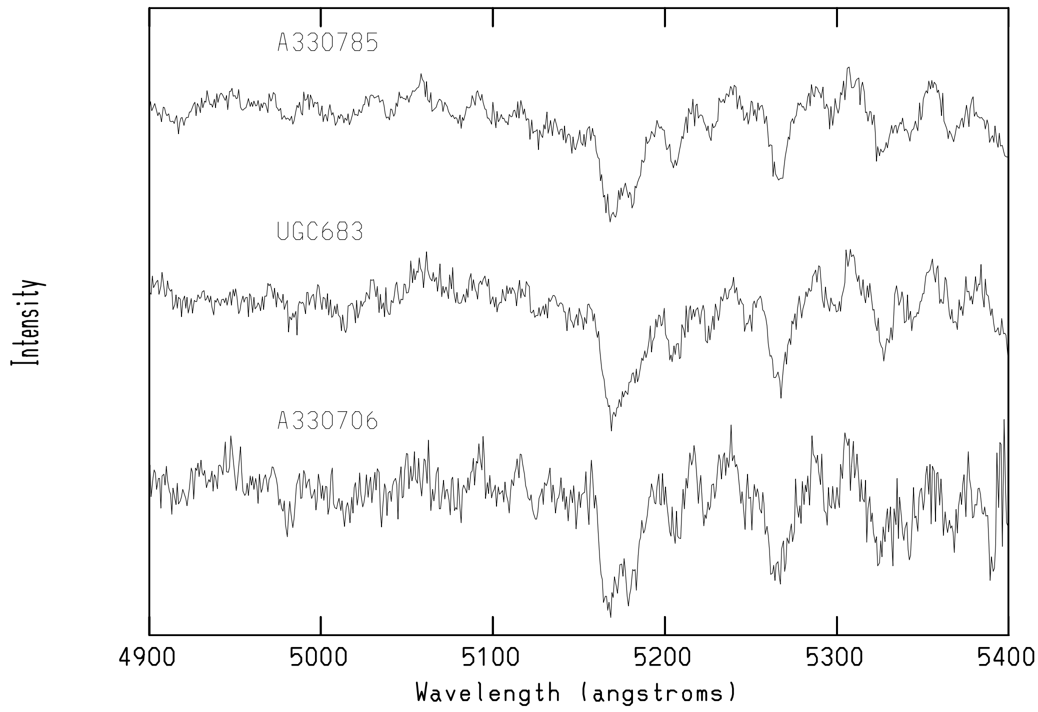

Fig. 1.— (Continued)

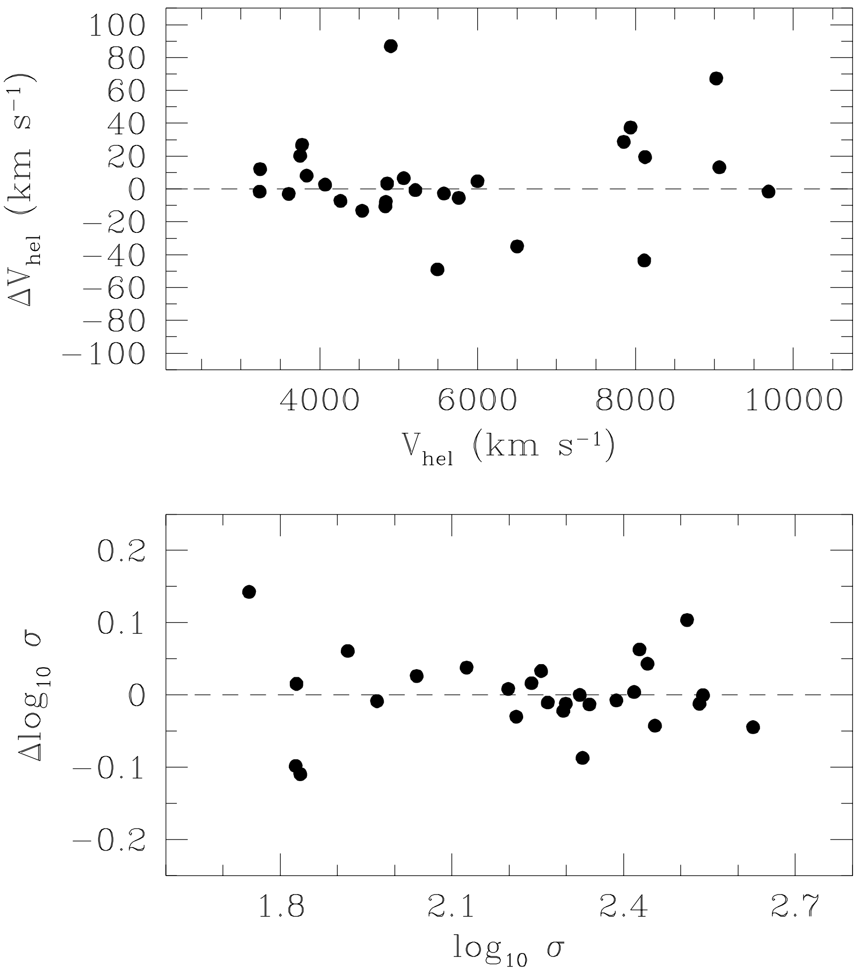

Fig. 2.— Internal comparison of the newly derived spectroscopic parameters. ΔV_{hel} and $\Delta log_{10}\sigma$ are the differences between the values of the heliocentric radial velocity and of the logarithm of the velocity dispersion obtained from repeated observations of 27 galaxies. They are plotted as a function of the mean value of the relative parameter, obtained combining the different measurements.

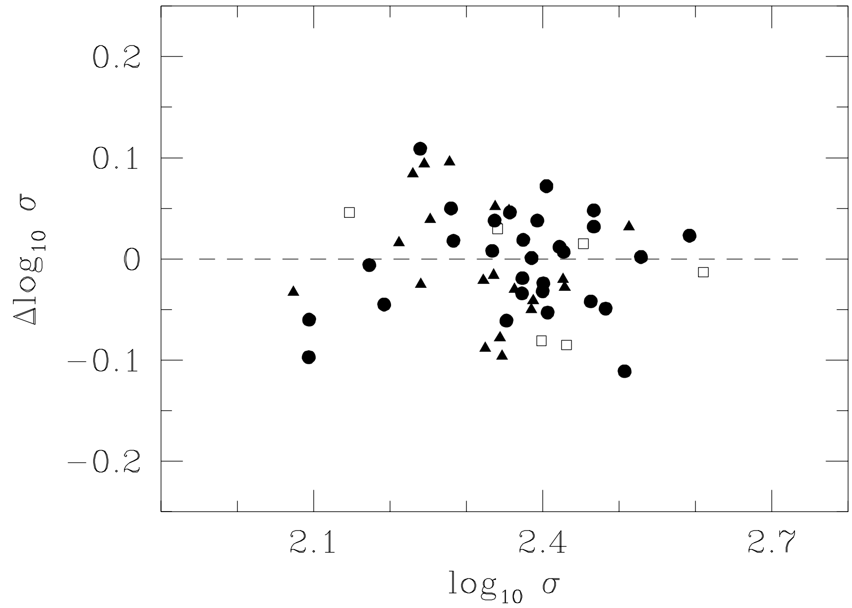

Fig. 3.— External comparison of the velocity dispersion measurements for galaxies in our sample. $\Delta log_{10}\sigma$ is the difference between the value of the logarithm of the velocity dispersion we obtained for a given galaxy, and the value found in the literature. This difference is plotted against mean value of this parameter, obtained combining the different measurements. Filled circles identify the comparison with the measurements of Faber *et al.* (1989), filled triangles the comparison with the measurements of Lucey *et al.* (1997), while open squares identify the comparison with the data of Lucey *et al.* (1991).